Orbital order in layered manganites probed with ^{57}Fe Mössbauer spectroscopy

Yutaka Ueda · Kiyoshi Nomura · Alexandre I. Rykov

Abstract In mixed-valence manganites, the doped iron species play the roles of simultaneous probes and ruiners for the orbital order occurring in the Mn-O electronic subsystem. We investigated the Mn^{3+}-based undoped system $RBaMn_2O_{5.5}$ and the half-doped systems $RBaMn_2O_6$, and $RBaMn_2O_5$ substituting a tiny portion of Mn^{3+} sites with Fe^{3+}. Single-site Mössbauer spectra were observed at room temperature in the charge-orbitally ordered state, i.e., below T_{COO}, for R=Y, Sm, Gd. Size of the rare earth ion strongly influences the quadrupole splitting in $RBaMn_2O_6$, but not in $RBaMn_2O_5$.

Keywords Mixed valence · Fe-doped manganites · A-site ordered perovskites · Mössbauer spectra · Effect of rare-earth ionic size on quadrupole splitting

1 Introduction

Charge and orbital order (COO) in manganites can melt under magnetic field, so that the material becomes metallic. Under application of very high magnetic fields the drop in resistance is colossal, however, smaller magnetic fields are sufficient to melt the less stable COO in manganites doped with Fe. In high-T_c (high-T_{COO})

Y. Ueda · A. I. Rykov
Institute for Solid State Physics, The University of Tokyo, 5-1-5 Kashiwanoha,
Kashiwa, 277-8581, Chiba, Japan

K. Nomura · A. I. Rykov
Graduate School of Engineering, The University of Tokyo, Hongo 7-3-1, 113-8656,
Tokyo, Japan

A. I. Rykov (✉)
Mössbauer Effect Data Center, Dalian Institute of Chemical Physics,
Chinese Academy of Sciences, 457 Zhongshan Road, Dalian 116023, China
e-mail: rykov@dicp.ac.cn

Fig. 1 Orbital order within one layer of $GdBaMn_2O_{5+y}$ ($y = 0$, 0.5 and 1). Filled states of the orbital e_g-doublet are depicted
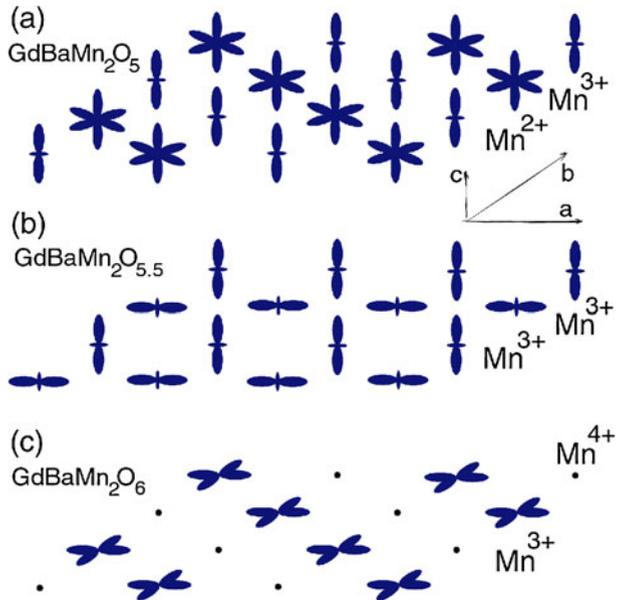
manganites, Fe doping at the level of 2% suppresses the value of T_{COO} by 40 or 50 K [1]. The value of T_{COO} monotonically decreases with increasing atomic size of rare earth, but remains above room temperature for such low doping levels as 2% of Fe (cf. $T_{COO} = 450$ K and $T_{COO} = 350$ K in $YBaMn_{1.96}Fe_{0.04}O_6$ and in $SmBaMn_{1.96}Fe_{0.04}O_6$, respectively). Thin films of such materials as $SmBaMn_2O_6$ are expected to show the gigantic and ultrafast responses arising from COO melting that makes these materials very attractive for correlated electron device technologies [2].

In the structure of the layered mixed-valence manganites $RBaMn_2O_{5+y}$ the large-size cations R^{3+} and Ba^{2+} form the separate layers alternating along c-axis with MnO_{1+y} layers. For the oxygen content ($5+y$) values of 5, 5.5 or 6 all the MnO_{1+y} layers are identical to each other. Each layer accommodates the charge and orbital order between Mn^{2+} and Mn^{3+} ($y = 0$), Mn^{3+} and Mn^{3+} ($y = 0.5$) and Mn^{3+} and Mn^{4+} ($y = 1$) shown in Fig. 1.

2 Experimental

Non-conventional multistep gas-heat-treatment procedures were used to synthesize these ^{57}Fe-doped powdered samples for R=La, Pr, Nd, Sm, Gd, Y. Integer-valued and half-integer-valued oxygen contents ($y = 0$, $y = 0.5$ and $y = 1$) in $RBaMn_2O_{5+y}$ are well-defined and isolated. They are stabilized owing to the orbital ordering of three different types shown in Fig. 1. However, easy sample annealing in reducing or oxidizing gas atmospheres may not lead to these orbitally ordered states. A-site disordered perovskites would result with no superstructure. Instead, in the A-site of the parent perovskite structure, the large-size cation R^{3+} and Ba^{2+} layered arrangement must be formed beforehand. The layered R-Ba superstructure becomes a crucial prerequisite for the orbital order of the Mn-O network. The layer-growing
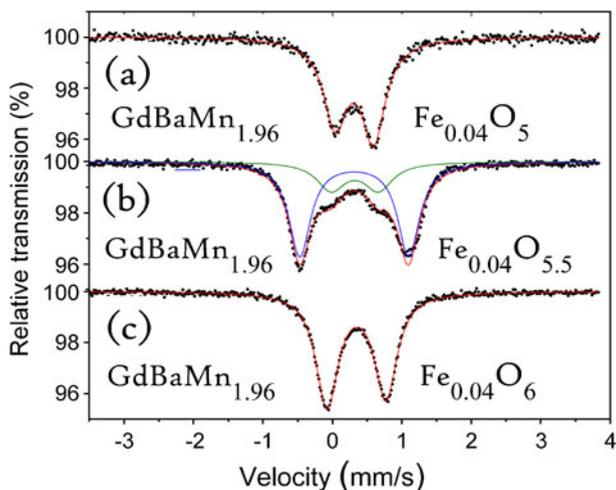
treatment in the clean reducing 6 N Ar atmosphere at 1,350°C was always necessary
to obtain the A-site ordered deoxygenated structures (y = 0) at the first synthesizing
step [3–5]. Subsequently, oxygenating and reducing treatments in layer-preserving
regimes at low temperature (~500°C) allowed varying only the oxygen contents and
related orbital arrangements within Mn-O layers.

3 Results and Discussion

When a small amount of manganese is substituted with iron we observe that all Fe
ions take the form of Fe^{3+}. All the Fe^{3+} ions reside in the sites of Mn^{3+}. This is not
surprising because the Mn^{3+} and Fe^{3+} ions are very similar in size. In contrast, the
site of Mn^{4+} is too small for Fe^{3+} and the site of Mn^{2+} is too large for Fe^{3+}.

Against the similarity of ionic sizes and charges, the orbital properties of the Mn^{3+}
and Fe^{3+} ions are very different. The Jahn-Teller (JT) ion Mn^{3+} tends to sit in a
low-symmetry environment. The symmetry degrades when only one of e_g orbitals is
half-filled. However, for Fe^{3+} ion both of the e_g orbitals are half-filled, so that the
semi-closed d-shell of Fe^{3+} is spherically symmetric. Unlike to the JT ions, such as
Mn^{3+} or Cu^{2+}, the ion Fe^{3+} have no valence contribution to the electric field gradient
(EFG) at the place of ^{57}Fe nuclei. Therefore, when Fe^{3+} is placed at the octahedral
site of Mn^{3+} the observed quadrupole splitting reproduces faithfully the distortion of
octahedral environment of Mn^{3+}.

In agreement with the number of the non-equivalent structural positions for Mn^{3+}
the Mössbauer spectra are single-site in oxygen-depleted (O_5) and oxygen-saturated
(O_6) samples, but show two doublets for the intermediate oxygen content (Fig. 2).
In the latter case, the major doublet comes from the site with the in-plane orientation
of the principal component of EFG. The minor subspectrum for y = 0.5, as well as
the spectra for y = 0 and y = 1 come from sites with out-of-plane orientation of the
main component of EFG ($V_{ZZ} \perp MnO_{1+y}$ planes).

Fig. 3 Dependence of the
room-temperature quadrupole
splitting on the volume of
reduced (perovskite-like) cell
in $RBaMn_2O_{5+y}$ ($y = 0$ and 1).
The symbol Sm1 denotes
the compounds
$Sm_{0.9}Nd_{0.1}BaMn_{1.96}Fe_{0.04}O_5$
and
$Sm_{0.9}Nd_{0.1}BaMn_{1.96}Fe_{0.04}O_6$
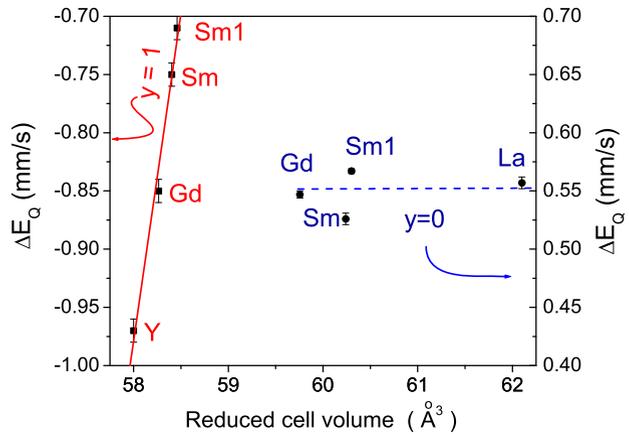
The 5-fold and 6-fold coordinations adopted by the Fe^{3+} ions are pyramidal in (a) and (b, minor doublet) and octahedral in (b, major doublet) and (c). Basically, they are the same as for Mn^{3+}. However, due to the difference of the orbital configurations of the Fe^{3+} and Mn^{3+} ions there appears some difference between the FeO_5 and MnO_5 pyramids [5]. Exact locations of the dopant Fe^{3+} and host Mn^{3+} inside of the pyramid do not coincide. The isotropic dopant ion Fe^{3+} is shifted towards the apex to equalize the fifth out-of-plane Fe-O distance with the four in-plane distances. In absence of such a shift we must expect much larger quadrupole splitting than observed.

Filling the in-plane orbital of the e_g-doublet in $RBaMn_2O_6$ (Fig. 1, c) induces in MnO_6 octahedra the strong vertical contraction that is reflected in the value of quadrupole splitting. The contraction is enhanced with smaller size of the rare earth R. Therefore, the absolute value of quadrupole splitting ΔE_Q increases when the volume of the reduced cell (perovskite-like cell) decreases (left-hand linear dependence in Fig. 3). On the other hand, in $RBaMn_2O_5$, where the thickness of the MnO_2 layer is determined mainly by the spherically symmetric ion Mn^{2+}, the value of ΔE_Q is roughly independent of the size of rare-earth ion R^{3+} (right-hand line in Fig. 3).

Asymmetry between the doublet line intensities arises mainly from platy habitus of layered crystals whose main surfaces are perpendicular to V_{ZZ}. The out-of-plane and in-plane 3d-orbitals are the half-filled orbitals of Mn^{3+} in the O_5 and O_6 cases, where $V_{ZZ} > 0$ and $V_{ZZ} < 0$, respectively. The opposite signs of V_{ZZ} results in opposite doublet asymmetries in Fig. 2 (a) and (c) owing to platy habits of microcrystals aligned in the plane of Mössbauer absorber. Additionally, a smaller asymmetry contribution exists owing to vibrational anisotropy. The total asymmetry is somewhat enhanced by this effect (Goldanskii–Karyagin) in O_6, but weakened in O_5 case [1, 6].

The orientation of V_{ZZ} along the vertical axis of the tetragonal P4/mmm modification [5] is obviously dictated for all R (except Y) in $RBaMn_2O_6$ by the axial site symmetry. The signs of V_{ZZ} are always confirmed by the ionic point charge model. Applying the ionic model to FeO_5 pyramid ($y = 0$), one expects the positive sign of V_{ZZ} as observed. For the octahedron ($y = 1$), strongly compressed along

vertical direction, the ionic model gives $V_{ZZ} < 0$. Although $YBaMn_2O_6$ undergoes monoclinic distortion at T_{COO}, this relatively small distortion has no effect on quadrupole splitting. As shown by linear fit in Fig. 3 and by our structure refinements, the vertical compression of octahedron increases quickly with decreasing the volume of perovskite cell; this strong compression continues to determine the value of quadrupole splitting even in presence of additional monoclinic distortion.

The fact that only one Mn^{3+} site exists in the cases of O_5 and O_6 Mössbauer spectra shows that the charge-ordered domains are configured under control of the frozen disorder of Fe. Random distribution of the Fe dopants tends to break down the ordered domains; however, the charge order would be reconstructed, centering all Mn^{3+} sites at Fe^{3+} ions. In contrast, two distinct Mn^{3+} sites exist in the $O_{5.5}$ phases synthesized at $1,450°C$ [5]. On cooling the iron dopants fall out preferentially into the octahedral sites of $GdBaMn_2O_{5.5}$, so that the population of pyramidal Fe species (inner doublet area) is found to be 4 times smaller.

References

1. Rykov, A.I., Ueda, Y., Nomura, K., Seto, M.: Phys. Rev. B **79**, 224114 (2009)
2. Ogimoto, Y., Nakamura, M., Harada, N., Ogawa, N., Miyano, K.: Math. Sci. Eng. B **173**, 51–56 (2010)
3. Millange, F., Caignaert, V., Domenges, B., Raveau, B.: Chem. Mater. **10**, 1974 (1998)
4. Nakajima, T., Kageyama, H., Ueda, Y.: J. Phys. Chem. Solids **63**, 913 (2002)
5. Rykov, A.I., Ueda, Y., Nomura, K.: J. Solid State Chem. **182**, 2157–2166 (2009)
6. Rykov, A.I., Seto, M., Ueda, Y., Nomura, K.: J. Appl. Crystallogr. **42**, 496–501 (2009)